Technical Report
RAL-TR-98-009

Density Profile Measurements of Non-Cylindrical Pulsed Gas Jets

TMR Large-Scale Facilities Access Programme

D Resendes et al

January 1998

COUNCIL FOR THE CENTRAL LABORATORY OF THE RESEARCH COUNCILS

Density Profile Measurements of Non-Cylindrical Pulsed Gas Jets

D Resendes et al

Instituto Superior Tecnico, Lisbon, Portugal

An experiment performed with funding from the

TMR Large-Scale Facilities Access Programme

Contract No. ERBFMGECT950053

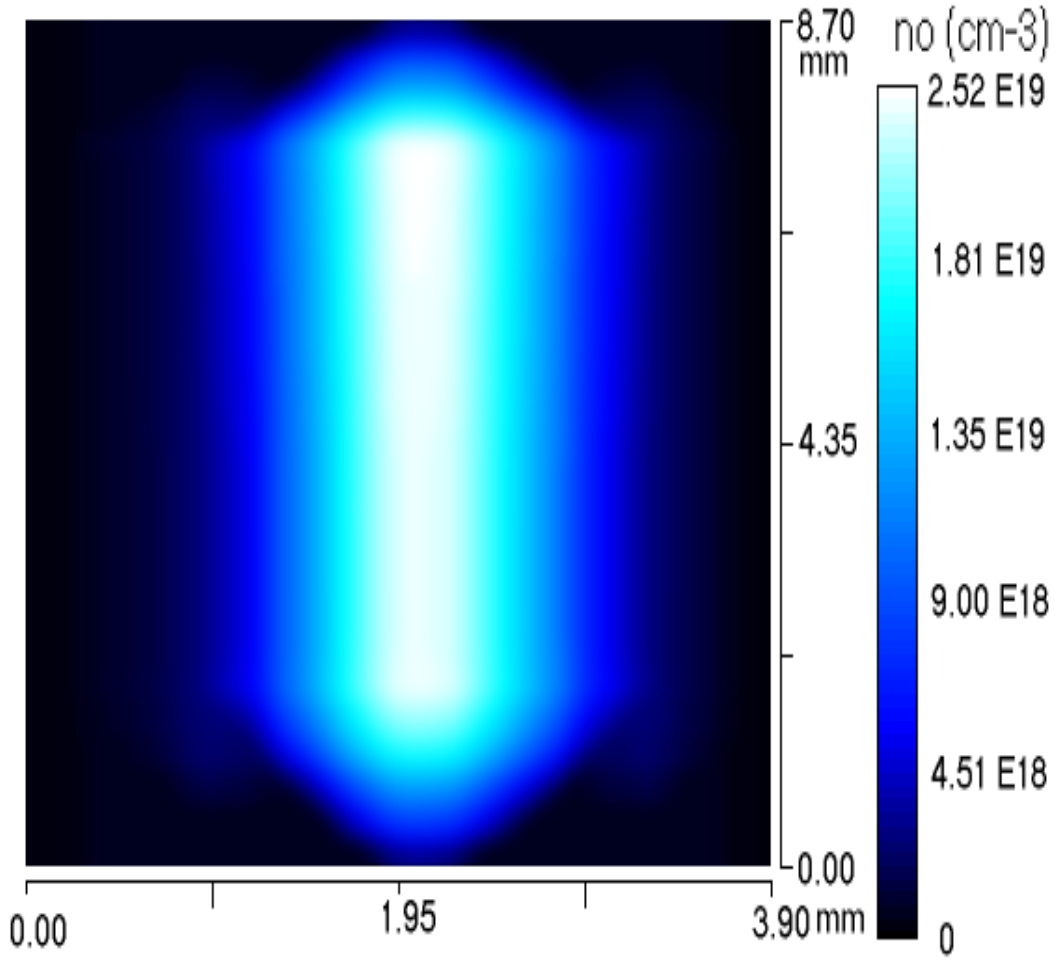

Density Profile Measurements of Non-Cylindrical Pulsed Gas Jets

An experiment performed with funding from the
TMR Large-Scale Facilities Access Programme

Access to Lasers at the Central Laser Facility
Rutherford Appleton Laboratory
Contract No. ERBFMGECT950053

D Resendes, R Azambuja, M Eloy, G Figueira

GoLP/Centro de Fisica de Plasmas, Instituto Superior Tecnico,
Av Rovisco Pais, 1096 Lisbon Codex, Portugal

D Neely
(Report prepared by CN Danson and G Booth)

Central Laser Facility, Rutherford Appleton Laboratory,
Chilton, Didcot, Oxon OX11 0QX, UK

SUMMARY

This report describes the experiment entitled 'Density Profile Measurements of Non-Cylindrical Pulsed Gas Jets'; carried out at the Central Laser Facility (CLF) from the 10th to the 23rd February 1997. The experiment, funded by the Framework IV Large-Scale Facilities Access Scheme, was proposed by Prof. D Resendes, GoLP/Centro de Fisica de Plasmas, Instituto Superior Tecnico, Lisbon, Portugal, and carried out by visiting researchers from the Institute. They were given technical support by researchers from the Central Laser Facility, Rutherford Appleton Laboratory.

Experimental Results

- We have fully characterised the three-dimensional density profile of non-cylindrical and cylindrical high-density pulsed gas jets by using a double orthogonal Mach-Zehnder interferometer and SART methods for inversion.
- The axial gas density decreases exponentially with the distance, z, from the nozzle tip with a scale length of approximately 1.4 mm and varies very little with time.
- With rectangular gas jets we obtain similar densities as those produced by cylindrical nozzles, but persisting for much longer lengths. Colliding two rectangular nozzles allows for even greater densities, without increasing the backing pressure.

Arising Publications

R Azambuja, M Eloy, G Figueira and D Neely. 'Three dimensional characterisation oh high-density non-cylindrical pulsed gas jets for laser-plasma interaction.' Central Laser Facility Annual Report, RAL-TR-97-045.

The CLF makes beam time at its facilities available to European Researchers with funding from DG-XII, CEC under the Large Scale Facilities Access Scheme. For further information contact Dr. Chris Edwards at the CLF. Tel: (0)1235 445582, e-mail: c.b.edwards@rl.ac.uk

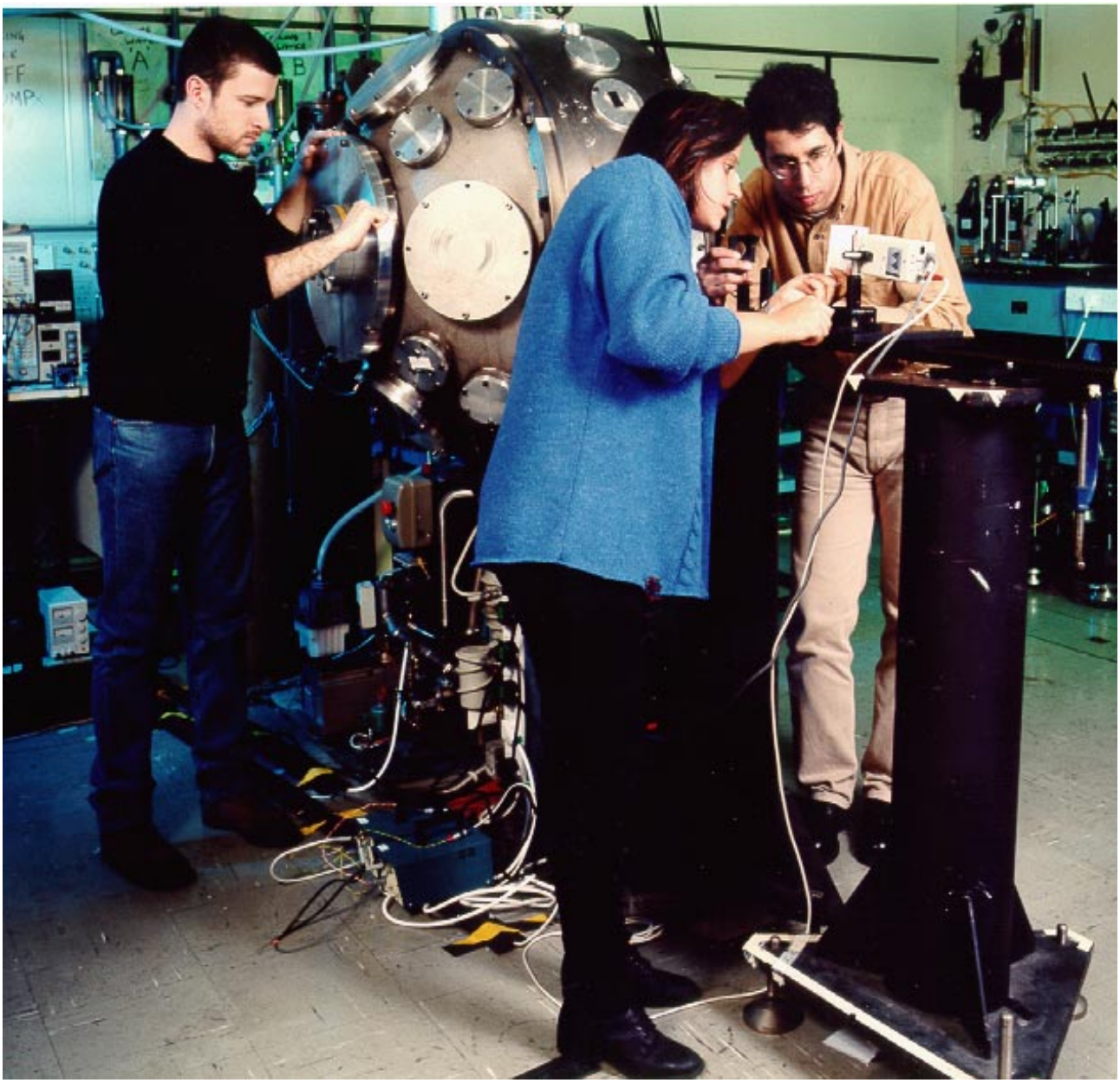

Researchers for the IST, Lisbon prepare the experimental area

From left to right: R Azambuja, M Eloy, G Figueira

Density Profile Measurements of Non-Cylindrical Pulsed Gas Jets

INTRODUCTION

Pulsed gas jets are commonly employed in a variety of research areas. Ionisation of such targets produces high electron density plasmas used in x-ray laser experiments[1-3] and laser-plasma interaction studies[4] . These kind of jets consist of either a spatially localised (<1mm) transversely uniform cylindrical column of neutral atoms in a low-density supersonic region or simple free-expansion jets extending for several millimetres in a high density gradient subsonic region, and have been fully characterised by several methods.[5-8]

For plasma-based acceleration schemes, such as the Laser Wakefield Accelerator (LWFA)[9-11], long regions (~ cm) of high electron density are required and can be achieved by using non-cylindrically symmetrical gas jets, such as rectangular-shaped nozzles. This geometry extends the interaction length and time between the pulse and the plasma and permits the creation of plasma channelling lengths at least one order of magnitude longer than those obtained with current cylindrical jets.

In the experiment described here we employed a double orthogonal Mach-Zehnder interferometer and Simultaneous Algebraic Reconstruction Technique (SART) algorithm to determine the three-dimensional density profile produced by rectangular nozzles of different dimensions and by the collision of two gas jets.

INVERSION METHODS - SART

Using interferometric techniques[12] we can determine the phase shift due to the propagation of a laser beam, with wavelength λ, through a medium, with refractive index n_o , by measuring the displacement of the interferogram fringes relative to their unperturbed position. The fringe shift, *h(j,z)*, as a percentage of the unperturbed interferogram, is:

$$h(j,z) = \frac{1}{\lambda}\int_L (n - n_0)\, d\alpha \qquad (1)$$

If we were to assume a cylindrically symmetric variation of the refractive index then *n(r)* could be determined using the inverse Abel transformation and a single projection of the object. However, in the case where no axial symmetries are present we must use tomographic methods and many projections. Several methods have been studied for image reconstruction. Literature[13,14] advises SART as the best choice of algorithm for the problem, with low-noise accurate image reconstruction and rapid convergence.

Methods of algebraic reconstruction (ART) in computer tomography are based on a representation of the projection line integrals as discrete ray-sums. The problem of reconstruction then becomes one of solving a system of linear equations of the form:

$$p_{mn} = \sum_{i=1}^{I} \sum_{j=1}^{J} w_{ijmn} f_{ij} \qquad (2)$$

For the unknown values of the image function f_{ij} on a sampling grid of size I x J, the solution will be expressed in terms of the given projection data p_{mn}. The subscript *m* represents the projection index from a total of *M* projections. The subscript *n* represents the ray index among *N* rays within each projection. The summation coefficients w_{ijmn} represent the area of the cell (i,j) covered by the ray (m,n).

The simultaneous algebraic reconstruction technique is an iterative method for solving the

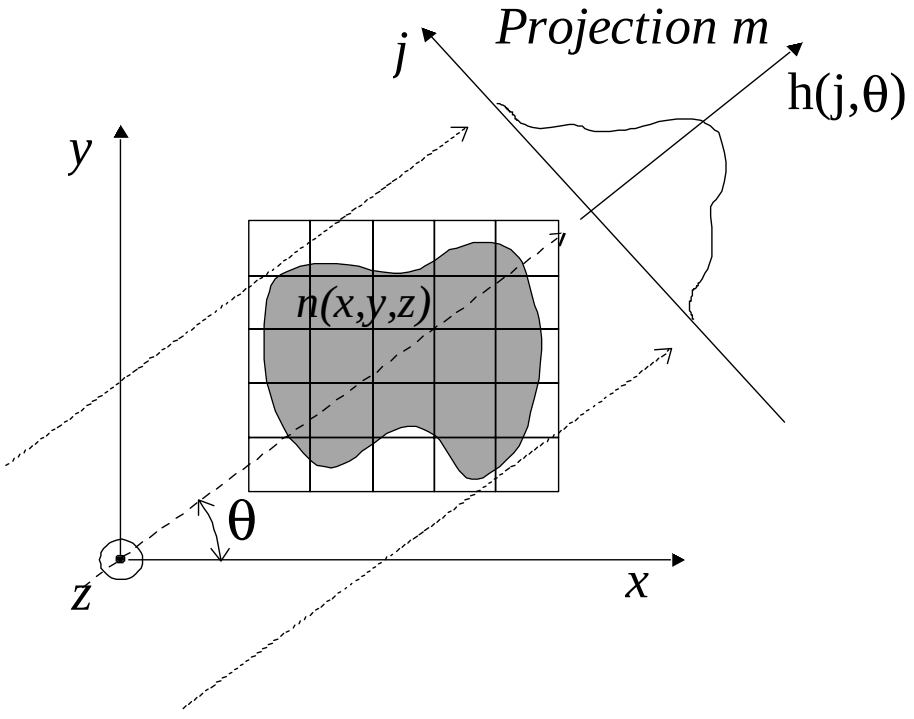

Fig 1. Cross Section of an assymmetrical phase object. The refractive

system of equations (2). Estimates $\hat{f}_{ij}^{(q)}$ of the image function f_{ij} are updated so as to satisfy the ray-sum equation (2). The new estimate $\hat{f}_{ij}^{(q+1)}$ is determined from the estimate $\hat{f}_{ij}^{(q)}$ by an update-correction strategy combining terms from all rays within a particular projection before the image function is updated, defined as:

$$\hat{f}_{ij}^{(q+1)} = \hat{f}_{ij}^{(q)} + \lambda^{(q)} \cdot \frac{\sum_{n=1}^{N} \left(w_{ijmn} \cdot \frac{p_{mn} - \sum_{i=1}^{I} \sum_{j=1}^{J} w_{ijmn} \hat{f}_{ij}^{(q)}}{\sum_{i=1}^{I} \sum_{j=1}^{J} w_{ijmn}} \right)}{\sum_{n=1}^{N} w_{ijmn}} \qquad (3)$$

One iteration of the algebraic reconstruction is complete when all ray-sum equations of the system have been used exactly once. The scaling factor $\lambda^{(q)}$ is a relaxation factor and its value can vary between two consecutive steps and projections and may be chosen in the range from 0.0 to 2.0. The initial estimate $\hat{f}_{ij}^{(q)}$ representing the point of departure for the reconstruction method is chosen as a zero function.

EXPERIMENTAL CONFIGURATION

A double orthogonal Mach-Zehnder interferometer consisting of four Al mirrors and four 50/50 beamsplitters of surface flatness $\lambda/20$ was mounted inside the Target Area 2 vacuum chamber.

The laser used was a low-power continuous-wave Green He-Ne (543nm) chopped at 50 Hz, giving rise to a pulse duration of 150 μs. Additional optics was employed for filtering, expanding and collimating the beam before entering the chamber. To ensure a smooth intensity variation, a diaphragm was used to apodise the beam contour.

The gas flow through the nozzle was controlled by a solenoid valve set to open for 4.8 ms connected to a high pressure N_2 reservoir at 900 psi. A He gas jet with equal backing pressure was also characterised. For every shot the chamber pressure was kept constant at 10^{-1} torr.

Interference patterns were registered using two free-running CCD cameras and recorded with a framestore (CEO) system. Both the solenoid valve and the framegrabber were triggered by a low-power, 50Hz-chopped, diode laser focused onto a photodiode and a digital delay generator.

Lenses with suitable focal lengths were used for imaging the gas jet zone onto the CCD sensors with different magnifications.

RESULTS AND CONCLUSION

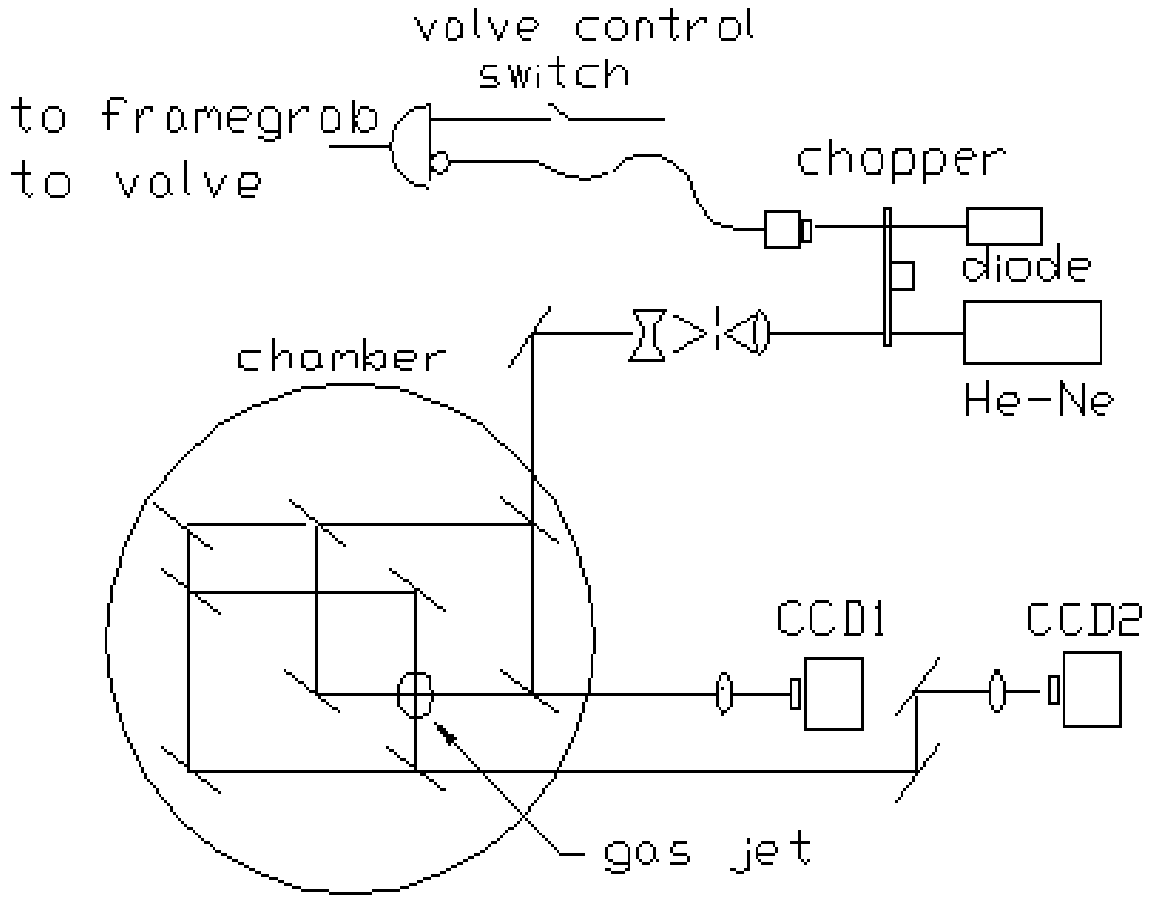

Fig 2. Experimental configuration.

We present the radial density profile obtained with N_2 for a cylindrical nozzle with diameter 1mm, (Figs. 3a., 3b.) for a rectangular nozzle, with dimensions 10 x 0.8mm^2 (Figs. 4a., 4b.) and for the collision of two nozzles with 5 x 0.65mm^2 and 5 x 1.1mm^2 (Figs. 5a., 5b), measured 28 milliseconds after the opening of the solenoid valve and for different distances, z, from the nozzle tip.

The axial gas density decreases exponentially with the distance, z, from the nozzle tip with a scale length of approximately 1.4 mm and varies very little with time as shown in Fig 6., for the rectangular nozzle.

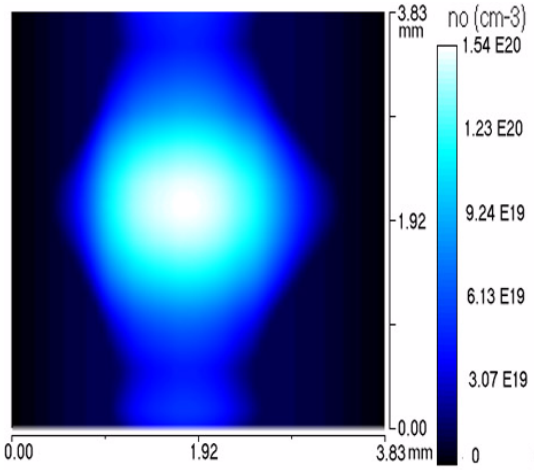

Fig 3a. Cylindrical nozzle,

z=500μm

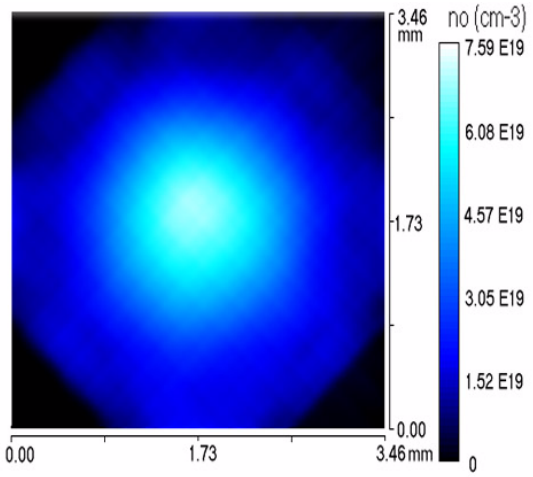

Fig 3b Cylindrical nozzle,

z=1000μm

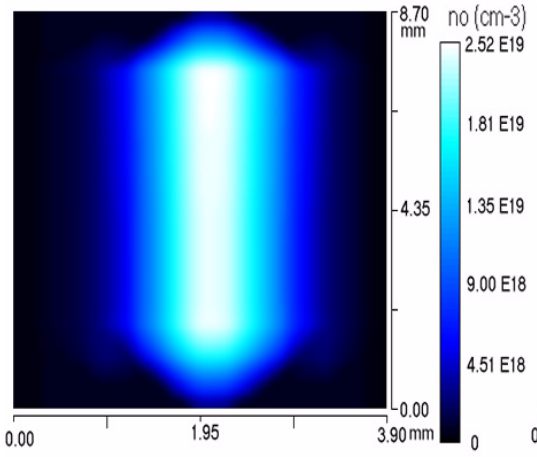

Fig4a. Rectangular nozzle,

z=505μm

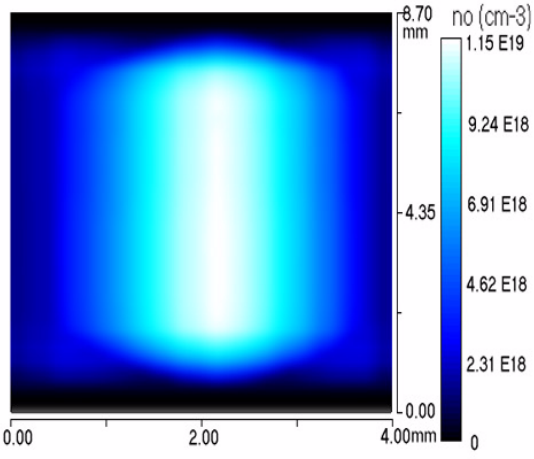

Fig4b. Rectangular nozzle,

z=1010 μm

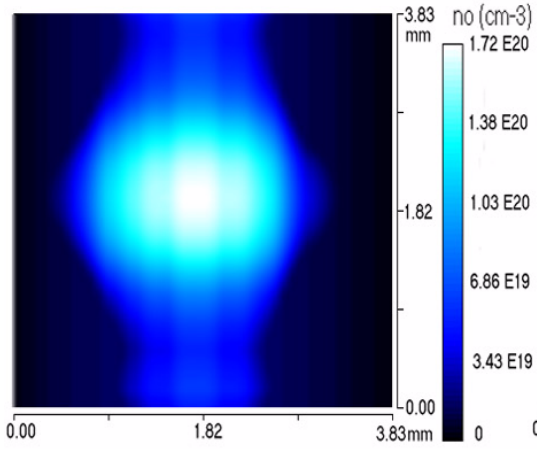

Fig5a. Two nozzle collision,

z=600 μm

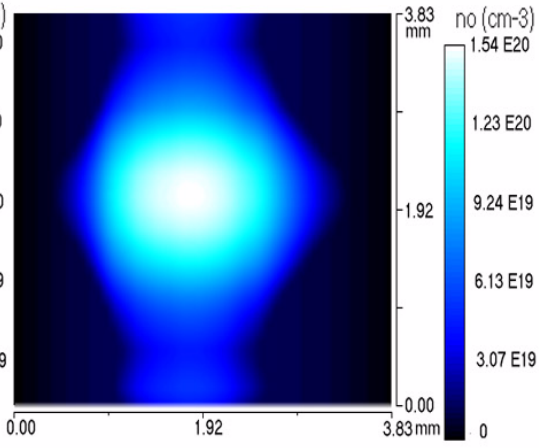

Fig5a. Two nozzle collision,

z=1200 μm

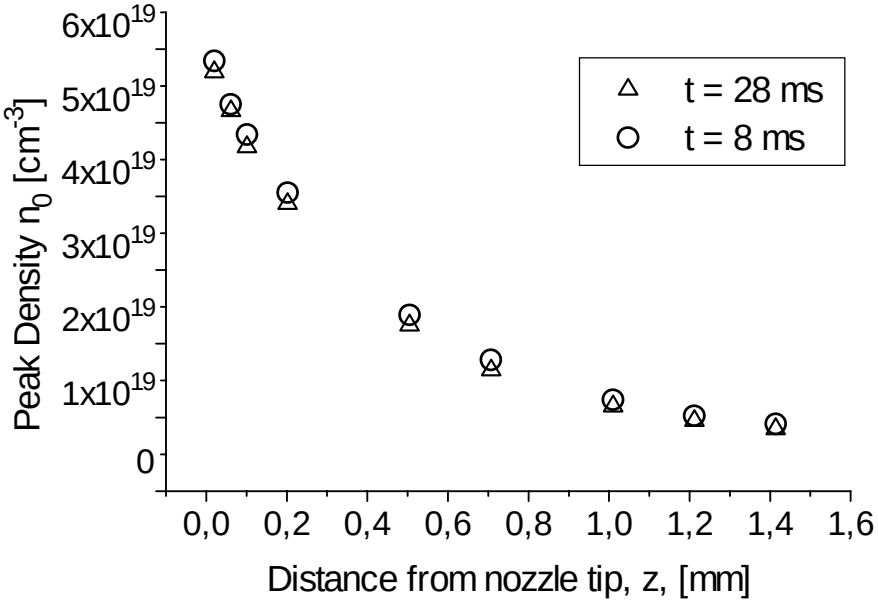

Fig 6.Peak density variation with distance from nozzle tip for two different instants after the opening of the solenoid valve.

We have fully characterised the three-dimensional density profile of non-cylindrical and cylindrical high-density pulsed gas jets by using a double orthogonal Mach-Zehnder interferometer and SART methods for inversion.

With rectangular gas jets we obtain similar densities as those produced by cylindrical nozzles, but persisting for much longer lengths. Colliding two rectangular nozzles allows for even greater densities, without increasing the backing pressure.

REFERENCES

1) N H Burnett and P B Corkum, J. Opt. Soc. Am. B, 6 1195, (1989)

2) N H Burnett and G D Enright, IEEE J. Quant. Electron , 26 1797, (1990)

3) H Fiedorowicz *et al.*, Phys. Rev. Lett., 76 415, (1996)

4) A Modena *et al.*, Nature, 377 606, (1995) and references therein

5) L Musinski *et al.*, Plasma Physics 24 731, (1982)

6) Y M Li and R Fedosejevs, Meas. Sci. Technol. 5 1197, (1994)

7) B Farizon *et al.*, Nuc. Inst. Meth. In Phys. Res. 101 287, (1995)

8) A Behjat, G J Tallents and D. Neely, CLF Annual Report (1996)

9) T Tajima and J M Dawson, Phys. Rev Lett. 43 267, (1979)

10) L M Gorbunov and V I Kirsanov, Zh. Eks. Teor. Fiz. 93 509, (1987) [Sov. Phys. JETP 93 260, (1987)]

11) P Sprangle *et al.* , Appl. Phys. Lett. 3 2146, (1988)

12) M Born and E Wolf, Principles of Optics, Pergamon Press (1970)

13) A H Andersen, IEEE Trans. on Med. Imag. 8 (1) 50, (1989) and references therein

14) R Gordon, IEEE Trans, on Med. Imag. (NS-21) 78, (1974)